Asian Journal of Chemistry; Vol. 37, No. 9 (2025), 2258-2264
ASIAN JOURNAL OF CHEMISTRY
https://doi.org/10.14233/ajchem.2025.34361

Biomolecule-Driven Supramolecular Gelation of Graphene Oxide: A Sustainable Route to Graphene–Metal Nanohybrid Gels with Catalytic Efficiency

ABHIJIT BISWAS

Department of Chemistry, Krishnagar Government College, Krishnagar-741101, India

Corresponding author: E-mail: biswas.abhijit5@gmail.com

Received: 28 June 2025 *Accepted*: 16 August 2025 *Published online*: 30 August 2025 AJC-22107

A sustainable and efficient approach has been developed for the fabrication of graphene-based nanohybrid gels *via* supramolecular gelation of graphene oxide (GO) using uric acid as a biologically relevant cross-linker. Gelation occurred under mild aqueous conditions through non-covalent interactions between uric acid and oxygenated functional groups on GO. The resulting GO-based gel was subsequently transformed into a graphene-based nanohybrid gel embedded with noble metal nanoparticles (Au, Ag) through *in situ* co-reduction using ascorbic acid as an environmentally benign reducing agent. Comprehensive structural and morphological analyses confirmed the retention of the gel network post-reduction and the uniform distribution of metal nanoparticles. Among the synthesized materials, the Au nanoparticle containing graphene-based gel exhibited excellent catalytic activity in the reduction of 4-nitrophenol, demonstrating high efficiency, structural stability and recyclability. This work presents a green and scalable strategy for developing functional soft materials, offering significant potential for applications in catalysis and nanomaterial-based technologies.

Keywords: Graphene, Uric acid, Green synthesis, Gel, Nanoparticles, Catalysis.

INTRODUCTION

Graphene oxide (GO), a free-standing two-dimensional (2D) crystal with atomic thickness, has emerged as a focal point of research across material science, biotechnology and nanotechnology domains [1]. Structurally, GO is an oxidized derivative of graphite comprising sp^2-hybridized carbon atoms arranged in a honeycomb network, resembling a true planar aromatic macromolecule [2]. Over the past decade, several methods have been developed for GO synthesis, including micro-mechanical exfoliation, chemical vapor deposition, epitaxial growth, and chemical oxidation of graphite [3,4]. Chemical reduction of GO produces reduced graphene oxide, often referred to as graphene. Graphene exhibits a unique set of physico-chemical properties, including high specific surface area, exceptional mechanical strength, excellent thermal conductivity and tunable electronic characteristics, which have positioned it as a versatile material for a wide range of applications [5-10]. Moreover, the emergence of graphene-based gels has further expanded the functional landscape of this material, enabling new possibilities in nanotechnology and soft matter research [11,12]. Gels are soft materials characterized by the immobilization of a liquid phase within a percolating solid-like network, formed *via* the self-assembly of molecular or supramolecular building blocks through non-covalent interactions such as hydrogen bonding, π–π stacking and electrostatic forces [13-15]. The fibrillar network in such gels provides a porous matrix capable of hosting nanoparticles and other nanomaterials [16-18]. The presence of hydrophilic functional groups (–OH, –COOH) and an extended polyaromatic surface enables GO to form gels in the presence of suitable interacting molecules under appropriate conditions. Numerous reports have described the synthesis of graphene-based gels and their applications in diverse areas [19-23]. For instance, Banerjee *et al.* [24] reported GO-based gels formed in the presence of amino acids or nucleosides. Kaliaraj *et al.* [25] developed a graphene-based nanocomposite gel with demonstrated efficacy in treating infectious wounds. Zhang *et al.* [26] synthesized functionalized graphene gels exhibiting excellent supercapacitive performance, while Peng *et al.* [27] designed smart graphene gels for endogenous stem cell-based regenerative therapy. The present study reports the formation of a graphene oxide-based supramolecular gel induced by the biologically active molecule, uric acid. Gelation occurs in

aqueous medium at room temperature and is driven by non-covalent interactions between uric acid and the hydrophilic functional groups (hydroxyl and carboxyl) present on the GO surface. This work highlights the potential of biologically relevant small molecules in the development of functional graphene-based soft materials. The uric acid-incorporated graphene oxide-based gel-phase materials have demonstrated remarkable versatility as nano-reactors for the *in situ* synthesis of metal nanoparticles, including gold (Au) and silver (Ag). Furthermore, graphene-based nanohybrid gels have been fabricated *via* the simultaneous reduction of metal ions and graphene oxide in the presence of another biologically active molecule, ascorbic acid (vitamin C), serving as the reducing agent. The strategic selection of gel components—namely, water as medium, graphene oxide and uric acid as gelator molecules and ascorbic acid as reductant enables precise control over the gel's reactivity. In this system, uric acid facilitates gelation through non-covalent interactions, while vitamin C promotes the reduction of both graphene oxide to graphene and metal salts to their corresponding nanoparticles within the gel matrix. Significantly, the resulting nanohybrid gel embedded with gold nanoparticles has been effecttively utilized as a reusable heterogeneous catalyst for the reduction of aromatic nitro compounds to amines under ambient conditions. The key advantage of this catalytic system lies in its facile separation from the reaction medium, which allows for multiple cycles of reuse without significant loss in catalytic activity, thereby highlighting the practical utility and robustness of the gold nanoparticle-containing nanohybrid gel.

EXPERIMENTAL

All analytical-grade chemicals utilized in this study were obtained from SRL, India. Natural graphite powder (particle size < 30 μm) and uric acid were procured from Sigma-Aldrich, India. Milli-Q ultrapure water was consistently used in all experimental procedures.

Synthesis of graphene oxide (GO): Graphene oxide was prepared from natural graphite powder by employing a modified Hummers and Offeman's protocol, as described in the literature [28].

Preparation of GO and graphene-based gel: A stock solution of uric acid (0.86 mg/mL) was prepared by dissolving it in Milli-Q water. Separately, a GO dispersion was obtained by dispersing GO in Milli-Q water at a concentration of 1.95 mg/mL, followed by thorough sonication to achieve a uniform viscous solution. Subsequently, 0.2 mL of uric acid solution was introduced into 0.8 mL of GO dispersion, and the mixture was sonicated to induce gelation. Sonication significantly accelerated the gel formation process, whereas in its absence, a considerably longer time was required for gelation. To convert the GO-based gel into a graphene-based gel, 0.2 mL of ascorbic acid solution (5 mg/ mL) was added and then system was heated at 80 ºC for several minutes, resulting in the formation of a graphene gel.

Synthesis of metal nanoparticles within graphene gel: To incorporate metal nanoparticles into the gel matrix, 50 μL of an aqueous solution of metal salt ($HAuCl_4/AgNO_3$; 2 mg/ mL) was first mixed with 0.8 mL of GO dispersion (5.8 mg/mL) and briefly sonicated. Subsequently, 0.2 mL of ascorbic acid solution (50 mg/mL) was added as a reducing agent, followed by the addition of 0.2 mL of uric acid solution (2.6 mg/mL). The mixture was then thoroughly sonicated to yield a graphene based gel embedded with metal nanoparticles. It is presumed that the metal ions were reduced in situ by ascorbic acid within the gel network, leading to the uniform formation of metal nanoparticles throughout the gel matrix.

Catalytic reduction study of 4-nitrophenol: In a standard catalytic experiment, 2.5 mL of an aqueous 4-nitrophenol solution (1.4×10^{-4} M) was mixed with 0.1 mL of freshly prepared $NaBH_4$ solution (0.1 M). Immediately after mixing, 1.26 g of wet graphene-based hybrid gel containing gold nanoparticles was introduced into the reaction mixture under continuous stirring. The reaction progress was monitored at regular time intervals using UV–Vis spectroscopy at room temperature. Upon completion of the reduction, the catalyst was retrieved using a spatula, thoroughly washed with Milli-Q water to remove any residual reactants, and air-dried. The recovered catalyst was reused in subsequent catalytic cycles.

Detection method: X-ray diffraction (XRD) analysis was performed on samples that were deposited onto glass substrates and air-dried at ambient conditions for several days. The measureements were carried out using a Bruker AXS diffractometer (Model D8 Advance) operating at 40 kV and 40 mA, equipped with a Ni-filtered Cu*K*α radiation source (λ = 1.54 Å). Prior to data acquisition, the instrument was calibrated using a standard corundum (Al_2O_3) reference. Data collection was executed using a LynxEye high-speed detector, with a scan rate of 0.3 sec and a step increment of 0.02˚. Rheological properties were assessed using a TA Instruments AR 2000 advanced rheometer with cone-plate geometry integrated into a Peltier temperature controlled stage. The cone used had a 40 mm diameter, a 1º59′50″ angle and a truncation gap of 56 μm. Frequency sweep measurements were conducted over a range of 0 to 120 rad/s at a constant strain amplitude of 0.01% under ambient temperature conditions. Transmission electron microscopy (TEM) was carried out by applying a small volume of the diluted gel-phase sample onto carbon- and Formvar-coated 300-mesh copper grids, followed by vacuum drying at room temperature for 48 h. Imaging was conducted using a JEOL transmittssion electron microscope operated at an accelerating voltage of 200 kV. Raman spectra were collected using a Horiba Jobin Yvon LABRAM HR 800 spectrometer with a laser excitation wavelength of 632.81 nm. UV–Visible absorption spectra, related to catalytic reduction studies, were recorded at room temperature using a Varian Cary 50 Bio UV–Vis spectrophotometer.

RESULTS AND DISCUSSION

Graphene oxide (GO) is a 2D nanostructure characterized by the presence of oxygen-rich functional groups such as hydroxyl and epoxide on its basal plane, along with carboxylic acid groups located at the sheet edges. These features enable GO to disperse uniformly in water, forming stable colloidal systems, primarily due to electrostatic repulsion between negatively charged sheets resulting from the ionization of carboxyl groups [29]. The functional groups, particularly –OH

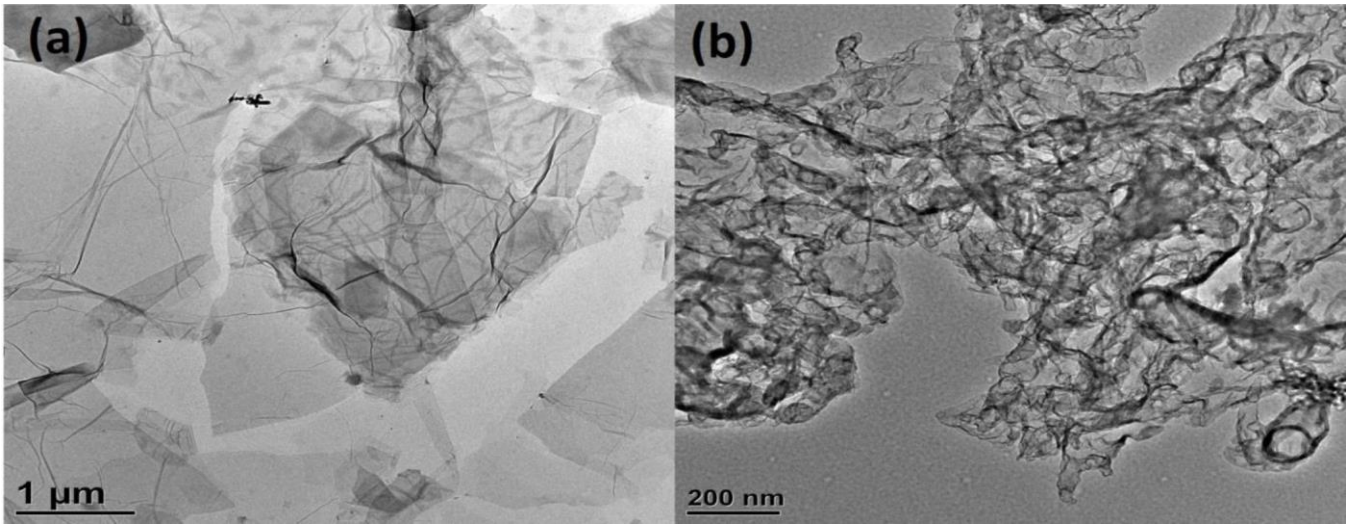

Fig. 1. HR-TEM images showing morphologies of (a) GO-based gel and (b) graphene-based gel

and –COOH, also allow for hydrogen bonding with compatible molecules, facilitating the formation of a gel-like network when appropriate cross-linkers/binders are introduced [29-31]. Herein, uric acid was employed as a molecular cross-linker to initiate gelation of GO in an aqueous medium. A typical preparation involved combining a GO suspension with a uric acid solution, followed by sonication, which subsequently led to the formation of a stable gel. This gel did not exhibit reversibility under thermal or mechanical stimuli. Uric acid, which contains nitrogen-based groups capable of engaging in hydrogen bonding, serves as a bridging agent between GO sheets through these non-covalent interactions. Water becomes entrapped within the interconnected GO–uric acid framework, leading to gel formation. The minimum gelation concentration (MGC) needed for gelation was found to be 0.26% (w/v), with an optimal uric acid-to-GO ratio of approximately 10% (w/w), indicating its high efficiency as a cross-linking agent.

Transformation of GO-based gel into graphene-based gel: The transformation of GO-based gel into a graphene-based gel can be effectively achieved through an *in situ* thermal reduction process employing vitamin C at 80 ºC. In this process, vitamin C serves as an effective and eco-friendly reducing agent, facilitating the conversion of GO to graphene within the gel matrix while preserving the overall gel integrity and network structure. TEM analysis (Fig. 1b) confirms the presence of nanostructured morphology in the graphene-based gel, indicating that the gel architecture remains intact post-reduction. Both the GO-based and graphene-based gels display self-assembled large nanosheets, cross-linked with one another to form a large 3D network like structure in the presence of cross-linker molecules. It is worth mentioning, the black lines visible in the TEM images of the graphene gel are attributed to the folding of graphene sheets, not nanofibers. This method is eco-friendly involving a non-toxic reagent and producing no gaseous byproducts. During the reduction process, a slight contraction of gel was observed, although the resulting graphene-based gel retains around 70% water content. This observed shrinkage is likely due to the decreased interlayer spacing associated with the reduction of GO to graphene.

The successful formation of graphene within the graphene-based gel matrix was confirmed through Raman spectroscopy, a reliable technique for analyzing carbon-based structures. The spectrum displayed two characteristic peaks at 1352 and 1595 cm^{-1}, corresponding to the D and G bands of graphene, respectively (Fig. 2). Significantly, the uric acid-containing gel exhibited a higher D/G intensity ratio, indicating an increased number of sp^2 carbon domains as a result of the reduction of GO within the gel phase.

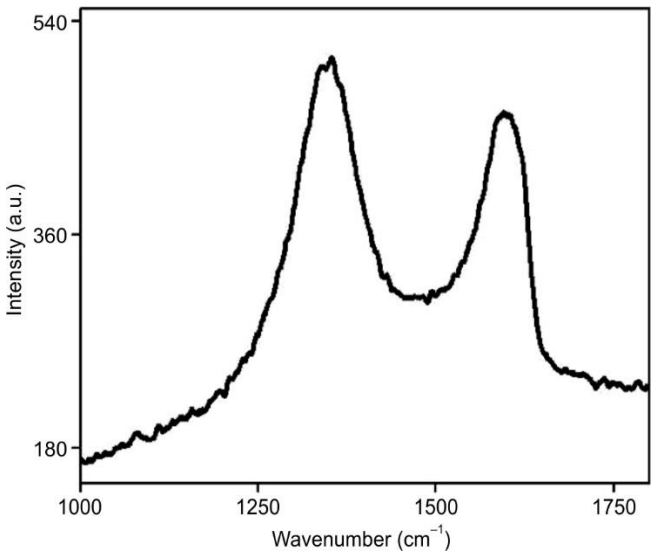

Fig. 2. Raman spectrum of a dried sample of a graphene-based gel

To assess the gel's viscoelastic nature, the rheological measurements were conducted at a fixed concentration of 1.26% (w/v) (Fig. 3). The storage modulus (G′) and loss modulus (G″) were recorded across a range of angular frequencies under a constant strain of 0.1%. In typical gel behaviour, G′ exceeds G″, while a transition to the sol state is marked by G′ falling below G″. At an angular frequency of 73.6 rad/s, the G′ values for the graphene-based and GO-based gels were 45.3 and 35.5 kPa, respectively, indicating enhanced mechanical strength in the graphene-based system. This increased strength is likely

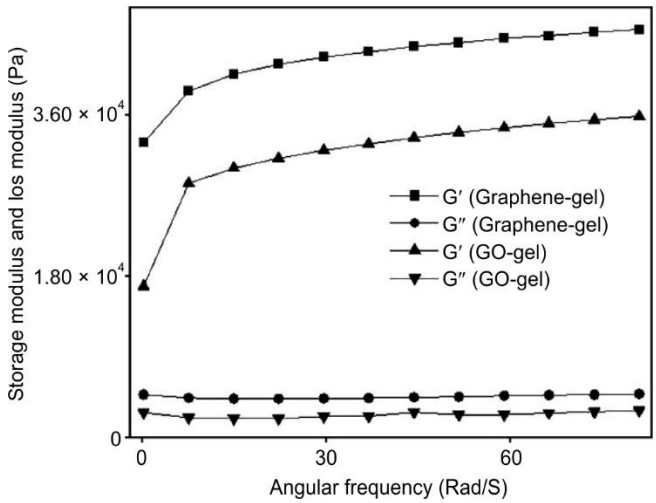

Fig. 3. Frequency-dependent dynamic storage modulus (G′) and loss modulus (G″) of GO-based gel and graphene-based gel, indicating their viscoelastic behaviour

due to the reduced interlayer spacing in graphene following GO reduction. Furthermore, in both gels, G′ consistently remained higher than G″ throughout the frequency range, highlighting the formation of a robust physical network. These results suggest that uric acid promotes effective gelation and enhances network rigidity by facilitating stronger intermolecular interactions.

Synthesis of metal nanoparticles containing graphene-based gel: Ascorbic acid is known for its ability to reduce various metal salts into their corresponding metal nanoparticles [32,33]. Leveraging this reducing capability, graphene-based nanohybrid gels embedded with metal nanoparticles (Au and Ag) were synthesized *via* an *in situ* co-reduction of metal ions and graphene oxide (Fig. 4). The successful formation of metal nanoparticles within the gel matrix was confirmed through X-ray diffraction (XRD) and transmission electron microscopy (TEM). XRD patterns of the Au-incorporated graphene gel (Fig. 5a) exhibited characteristic reflections at 2θ = 38.31º, 44.41º, 64.44º and 77.88º corresponding to the (111), (200), (220) and (311) planes of Au, respectively. Similarly, distinct peaks at 2θ value of about 38.2º, 44.1º, 64.8º and 78.0º were observed for silver, corresponding to (111), (200), (220) and (311) planes of silver (Fig. 5b). Both nanohybrid gels displayed an additional peak around 2θ = 22.8°, indicative of the reduction of GO to graphene within the gel matrix.

Further characterization using TEM, selected area electron diffraction (SAED) and energy-dispersive X-ray (EDX) spectroscopy supported the presence and morphology of the metal nanoparticles. TEM images (Fig. 6a,d) revealed the spherical nanoparticles uniformly distributed over the graphene nano-

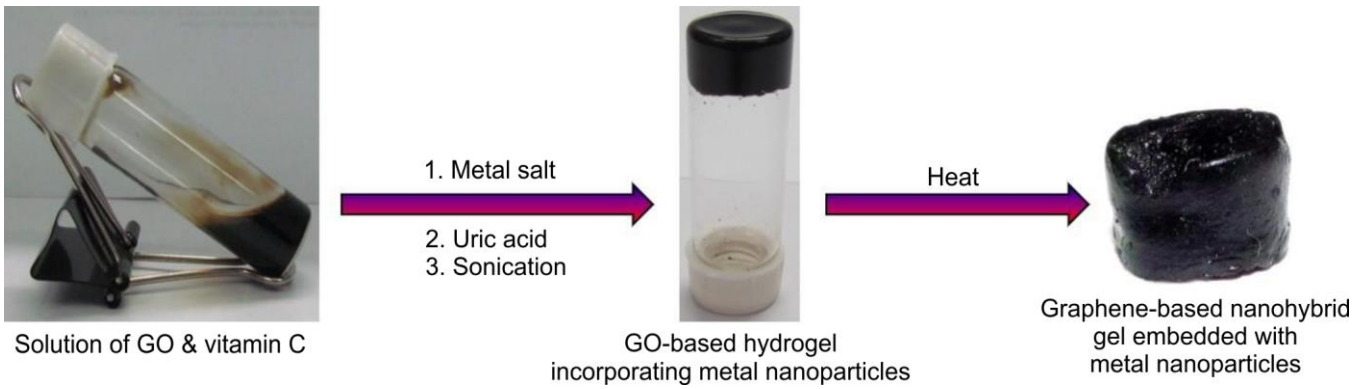

Fig. 4. Schematic illustration of the formation of a graphene-based nanohybrid gel embedded with metal nanoparticles

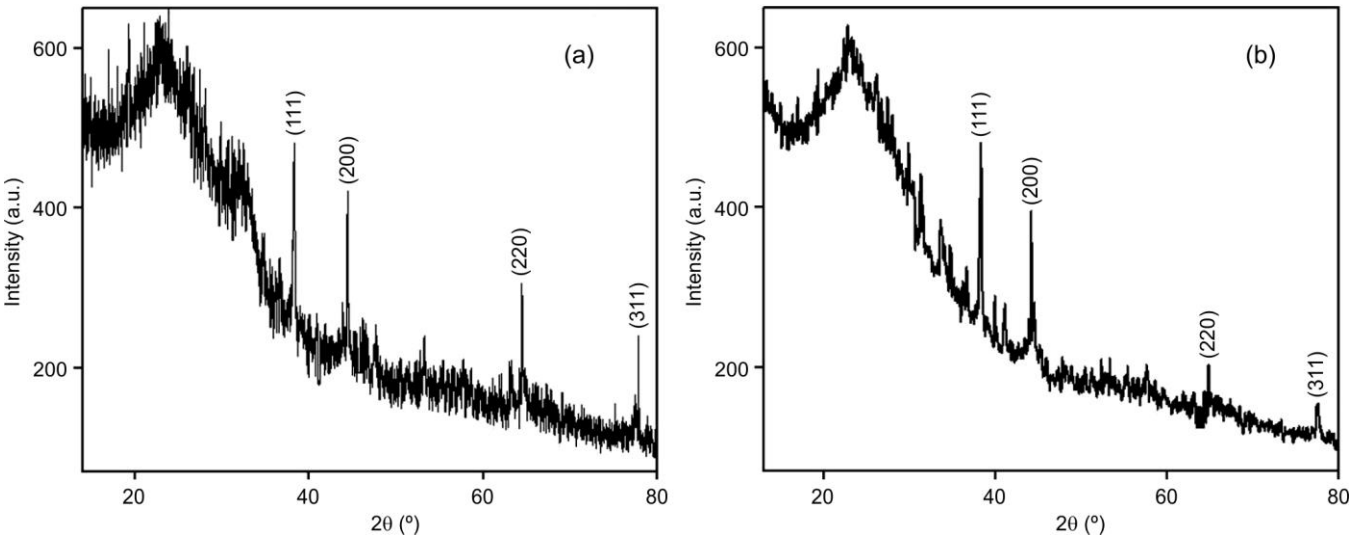

Fig. 5. X-ray diffraction (XRD) patterns of graphene-based nanohybrid gels containing (a) Au nanoparticles and (b) Ag nanoparticles

sheets. The uniform and homogenous decoration of metal nanoparticle on the graphene nanosheets can be due to *in situ* reduction of metal salts within the gel matrix. Moreover, the free space within the 3D cross-linked gel framework likely facilitated nanoparticle nucleation and growth. The average particle sizes were estimated from TEM images to be approximately 13 nm for Au and 17 nm for Ag nanoparticles. EDX spectra (Fig. 6b,e) confirmed the elemental composition and SAED patterns (Fig. 6c,f) exhibited concentric diffraction rings corresponding to the crystalline nature of the embedded Au and Ag nanoparticles.

Catalytic activities: Graphene-supported metal nanoparticle based materials have gained significant attention in catalysis owing to their high surface area, excellent electron mobility and superior mechanical robustness [34-36]. In this study, a self-standing, gold metal nanoparticle-embedded graphene-based gel was used as an efficient and reusable nanocatalyst. The catalytic performance of the gold nanoparticle-incorporated gel was evaluated through the reduction of 4-nitrophenol in presence of sodium borohydride ($NaBH_4$). For this, a freshly prepared aqueous $NaBH_4$ solution was added to a diluted aqueous solution of 4-nitrophenol. Upon addition of $NaBH_4$, the absorption peak of 4-nitrophenol shifted to 400 nm, attributed to the formation of the phenoxide ion rather than the reduction of the nitro group. The catalytic reaction was monitored over time using UV–Vis spectroscopy in the presence of the hybrid gel catalyst. A gradual decrease in the absorbance at 400 nm, along with a simultaneous increase at 297 nm (Fig. 7a), corresponding to 4-aminophenolate, confirmed the efficient catalytic reduction. Upon completion, the 400 nm peak disappeared completely, accompanied by a visible colour change from yellowish-green to colourless. The rate constant (k) for the reaction was calculated as 8.09×10^{-2} min^{-1} (Fig. 7b). Notably, the catalytic activity remained largely unaffected over multiple reaction cycles, indicating the high reusability of the catalyst. This sustained performance is attributed to the intact gel structure, which allowed easy recovery of the catalyst from the reaction mixture without significant loss. Furthermore, the extended π-conjugated surface of the graphene sheets facilitated strong π–π interactions with the reactant molecules, thereby enhancing their local concentration near the embedded nanoparticles and promoting catalytic efficiency.

Conclusion

A straightforward and environmentally benign strategy was developed for the synthesis of nanohybrid systems using a graphene-based gel as a nanoreactor. In this approach, uric acid, a biologically relevant molecule was employed as a cross-linking agent to induce gelation of GO, resulting in a GO-based supramolecular gel. This gel was subsequently converted into a noble metal nanoparticle-embedded graphene-based nano-

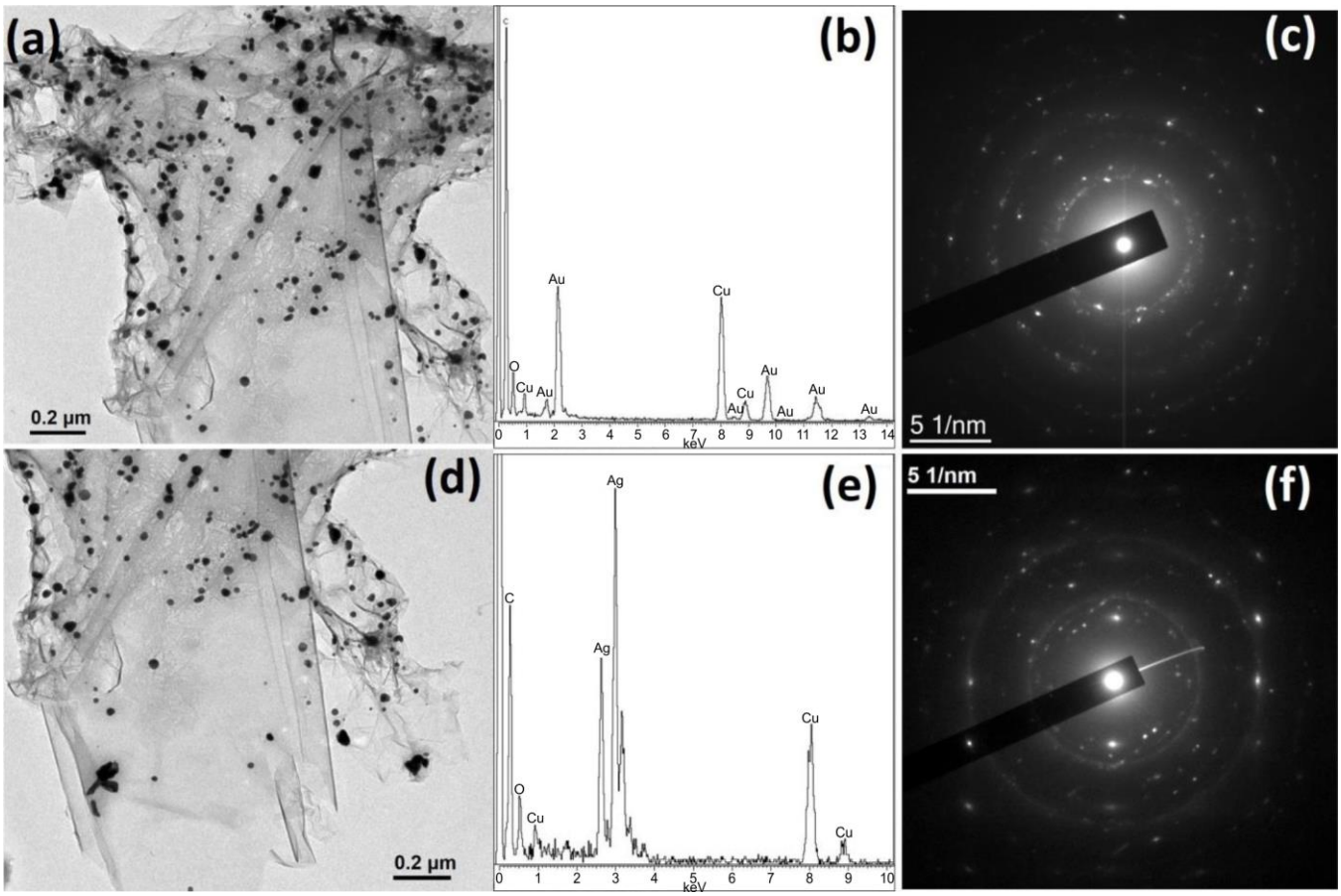

Fig. 6. TEM images of (a) Au and (d) Ag nanoparticles containing graphene-based gel; EDX analyses of metal nanoparticle containing graphene-based gel showing the presence of (b) Au and (e) Ag nanoparticles; SAED patterns of (c) Au and (f) Ag nanoparticles supported on the graphene-based gel matrix

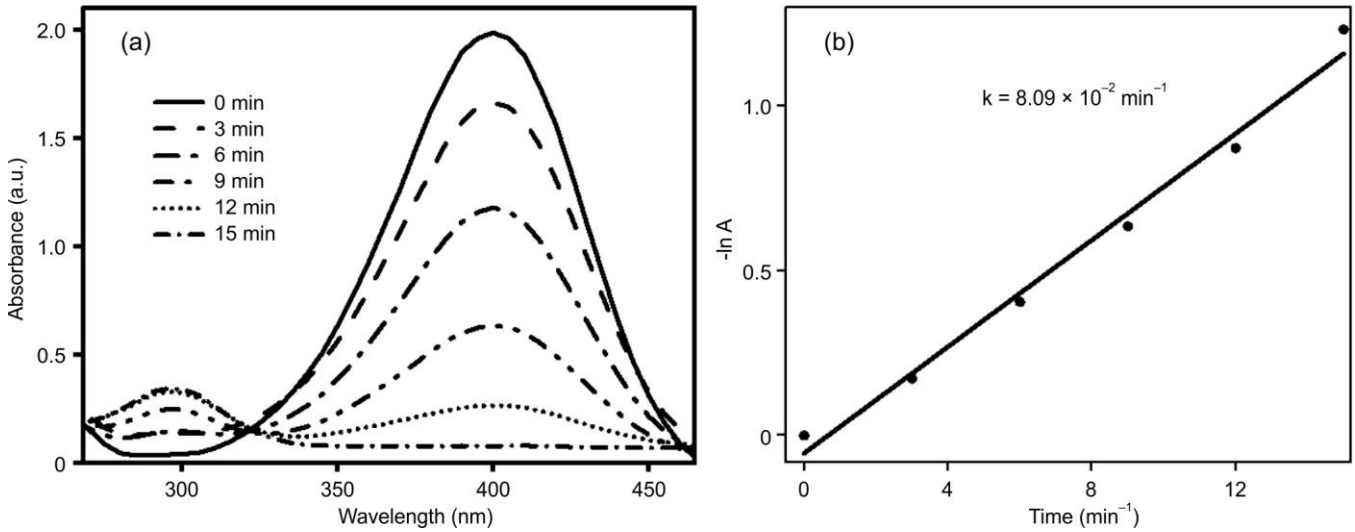

Fig. 7. (a) UV-Vis spectra showing the catalytic reduction of 4-nitrophenol in the presence of the catalyst; (b) Plot for the calculation of the rate constant of the reaction based on the time-dependent absorbance data

hybrid gel through an *in situ*, simultaneous co-reduction of both GO sheets and metal precursors (Au and Ag) using ascorbic acid (vitamin C) as a mild, non-toxic reducing agent. The morphological analysis revealed that the gel retained its interconnected network-like architecture even after the reduction process. Among the resulting materials, the graphene gel embedded with Au nanoparticles served as a highly effective catalyst for the reduction of 4-nitrophenol. The as-synthesized nanohybrid gel catalyst offered several distinct advantages like (i) utilization of inexpensive, eco-friendly reagents; (ii) high structural and catalytic stability during the reaction; and (iii) ease of separation from the reaction medium, enabling effective recyclability. The entire process exemplifies a sustainable and green synthetic route, free from hazardous reagents. This nanohybrid gel platform presents a promising foundation for the development of advanced gel-based functional materials with potential applications across various fields.

ACKNOWLEDGEMENTS

The author extends heartfelt his appreciation to Krishnagar Government College, Krishnagar, India, for their generous provision of research resources. Furthermore, gratitude is also expressed to the Indian Association for the Cultivation of Sciences (IACS), India, for their invaluable support in granting access to the instrumental facilities and their extensive library resources.

CONFLICT OF INTEREST

The authors declare that there is no conflict of interests regarding the publication of this article.

REFERENCES

1. K. Geim, *Science*, **324**, 1530 (2009); https://www.science.org/doi/10.1126/science.1158877
2. R. Ruoff, *Nat. Nanotechnol.*, **3**, 10 (2008); https://doi.org/10.1038/nnano.2007.432
3. B. Anegbe, I.H. Ifijen, M. Maliki, I.E. Uwidia and A.I. Aigbodion, *Environ. Sci. Eur.*, **36**, 15 (2024); https://doi.org/10.1186/s12302-023-00814-4
4. D. Chen, H. Feng and J. Li, *Chem. Rev.*, **112**, 6027 (2012); https://doi.org/10.1021/cr300115g
5. A.H. Castro Neto, F. Guinea, N.M.R. Peres, K.S. Novoselov and A.K. Geim, *Rev. Mod. Phys.*, **81**, 109 (2009); https://doi.org/10.1103/RevModPhys.81.109
6. A.K. Geim and K.S. Novoselov, *Nat. Mater.*, **6**, 183 (2007); https://doi.org/10.1038/nmat1849
7. D. Chen, L. Tang and J. Li, *Chem. Soc. Rev.*, **39**, 3157 (2010); https://doi.org/10.1039/b923596e
8. M.D. Stoller, S. Park, Y. Zhu, J. An and R.S. Ruoff, *Nano Lett.*, **8**, 3498 (2008); https://doi.org/10.1021/nl802558y
9. C. Lee, X. Wei, J.W. Kysar and J. Hone, *Science*, **321**, 385 (2008); https://doi.org/10.1126/science.1157996
10. A.A. Balandin, S. Ghosh, W. Bao, I. Calizo, D. Teweldebrhan, F. Miao and C.N. Lau, *Nano Lett.*, **8**, 902 (2008); https://doi.org/10.1021/nl0731872
11. S. Hussain, *Results Chem.*, **6**, 101029 (2023); https://doi.org/10.1016/j.rechem.2023.101029
12. Y. Lei, T. Zhang, Y.-C. Lin, T. Granzier-Nakajima, D.A. Kowalczyk, G. Bepete, Z. Lin, D. Zhou, T. F. Schranghamer, Y. Chen, A. Dodda, A. Sebastian, G. Pourtois, T.J. Kempa, B. Schuler, M.T. Edmonds, Y. Liu, S.Y. Quek, U. Wurstbauer, S.M. Wu, N.R. Glavin, S. Das, S.P. Dash, J.M. Redwing, J.A. Robinson and M. Terrones, *ACS Nanosci. Au*, **2**, 450 (2022); https://doi.org/10.1021/acsnanoscienceau.2c00017
13. K.Y. Lee and D.J. Mooney, *Chem. Rev.*, **101**, 1869 (2001); https://doi.org/10.1021/cr000108x
14. A.R. Hirst, B. Escuder, J.F. Miravet and D.K. Smith, *Angew. Chem. Int. Ed.*, **47**, 8002 (2008); https://doi.org/10.1002/anie.200800022
15. X. Li, K. Yi, J. Shi, Y. Gao, H.-C. Lin and B. Xu, *J. Am. Chem. Soc.*, **133**, 17513 (2011); https://doi.org/10.1021/ja208456k
16. S. Sheikh-Oleslami, B. Tao, J. D'Souza, F. Butt, H. Suntharalingam, L. Rempel and N. Amiri, *Gels*, **9**, 591 (2023); https://doi.org/10.3390/gels9070591
17. H.-L. Tan, S.-Y. Teow and J. Pushpamalar, *Bioengineering*, **6**, 17 (2019); https://doi.org/10.3390/bioengineering6010017
18. O. Gazil, D. Alonso Cerrón-Infantes, N. Virgilio and M.M. Unterlass, *Nanoscale*, **16**, 17778 (2024); https://doi.org/10.1039/D4NR00581C
19. L.M.T. Phan, T.A.T. Vo, T.X. Hoang and S. Cho, *Nanomaterials*, **11**, 906 (2021); https://doi.org/10.3390/nano11040906

20. J. Jing, X. Qian, Y. Si, G. Liu and C. Shi, *Molecules*, **27**, 924 (2022); https://doi.org/10.3390/molecules27030924
21. Y. Kim, R. Patel, C.V. Kulkarni and M. Patel, *Gels*, **9**, 967 (2023); https://doi.org/10.3390/gels9120967
22. H. Lu, S. Zhang, L. Guo and W. Li, *RSC Adv.*, **7**, 51008 (2017); https://doi.org/10.1039/C7RA09634H
23. Y. Ni Chen, Z. Wang, X. Zhang, F. Gao, Z. Shao and H. Wang, *J. Tissue Eng.*, **15**, 1 (2024); https://doi.org/10.1177/20417314241282
24. B. Adhikari, A. Biswas and A. Banerjee, *Langmuir*, **28**, 1460 (2012); https://doi.org/10.1021/la203498j
25. D.K. Shanmugam, Y. Madhavan, A. Manimaran, G.S. Kaliaraj, K.G. Mohanraj, N. Kandhasamy and K.K. Amirtharaj Mosas, *Gels*, **9**, 22 (2022); https://doi.org/10.3390/gels9010022
26. Y. Zhang, C.-G. Zhou, X.-H. Yan, Y. Cao, H.-L. Gao, H.-W. Luo, K.-Z. Gao, S.-C. Xue and X. Jing, *J. Power Sources*, **565**, 232916 (2023); https://doi.org/10.1016/j.jpowsour.2023.232916
27. C. Zhang, T.-J. Yuan, M.-H. Tan, X.-H. Xu, Y.-F. Huang and L.-H. Peng, *Biomater. Sci.*, **9**, 2146 (2021); https://doi.org/10.1039/D0BM01963A
28. W. Hummers Jr. and R.E. Offeman, *J. Am. Chem. Soc.*, **80**, 1339 (1958); https://doi.org/10.1021/ja01539a017
29. X. Zhang, Z. Sui, B. Xu, S. Yue, Y. Luo, W. Zhan and B. Liu, *J. Mater. Chem.*, **21**, 6494 (2011); https://doi.org/10.1039/c1jm10239g
30. A.H. Hung, R.J. Holbrook, W. Rotz, C.J. Glasscock, N.D. Mansukhani, K.W. MacRenaris, L.M. Manus, M.C. Duch, K.T. Dam, M.C. Hersam and T.J. Meade, *ACS Nano*, **8**, 10168 (2014); https://doi.org/10.1021/nn502986e
31. Y. Xu, Q. Wu, Y. Sun, H. Bai and G. Shi, *ACS Nano*, **4**, 7358 (2010); https://doi.org/10.1021/nn1027104
32. L. Malassis, R. Dreyfus, R.J. Murphy, L.A. Hough, B. Donnio and C.B. Murray, *RSC Adv.*, **6**, 33092 (2016); https://doi.org/10.1039/C6RA00194G
33. D. Singha, N. Barman and K. Sahu, *J. Colloid Interface Sci.*, **413**, 37 (2014); https://doi.org/10.1016/j.jcis.2013.09.009
34. M.B. Burkholder, F.B.A. Rahman, E.H. Chandler Jr., J.R. Regalbuto, B.F. Gupton and J.M.M. Tengco, *Carbon Trends*, **9**, 100196 (2022); https://doi.org/10.1016/j.cartre.2022.100196
35. B.F. Machado and P. Serp, *Catal. Sci. Technol.*, **2**, 54 (2012); https://doi.org/10.1039/C1CY00361E
36. H.-Y. Zhuo, X. Zhang, J.-X. Liang, Q. Yu, H. Xiao and J. Li, *Chem. Rev.*, **120**, 12315 (2020); https://doi.org/10.1021/acs.chemrev.0c00818